



PyReconstruct: A fully open-source, collaborative successor to Reconstruct

Michael A. Chirillo^{a,1}, Julian N. Falco^{a,1}, Michael D. Musslewhite^a, Larry F. Lindsey^a, and Kristen M. Harris^{a,2}

Affiliations are included on p. 11.

Contributed by Kristen M. Harris; received March 14, 2025; accepted June 22, 2025; reviewed by Helen Barbas, R. Anne McKinney, and Pat K. Rivlin

As the serial section community transitions to volume electron microscopy, tools are needed to balance rapid segmentation efforts with documenting the fine detail of structures that support cell function. New annotation applications should be accessible to users and meet the needs of the neuroscience and connectomics communities while also being useful across other disciplines. Issues not currently addressed by a single, modern annotation application include 1) built-in curation systems with utilities for expert intervention to provide quality assurance, 2) integrated alignment features that allow for image registration on-the-fly as image flaws are found during annotation, 3) simplicity for nonspecialists within and beyond the neuroscience community, 4) a system to store experimental metadata with annotation data in a way that researchers remain masked regarding condition to avoid potential biases, 5) local management of large datasets appropriate for circuit-level analyses, and 6) fully open-source codebase allowing development of new tools, and more. Here, we present PyReconstruct, a modern successor to the Reconstruct annotation tool. PyReconstruct operates in a field-agnostic manner, runs on all major operating systems, breaks through legacy RAM limitations, features an intuitive and collaborative curation system, and employs a flexible and dynamic approach to image registration. It can be used to analyze, display, and publish experimental or connectomics data. PyReconstruct is suited for generating ground truth to implement in automated segmentation, outcomes of which can be returned to PyReconstruct for proofreading and quality control.

annotation | software | opensource | reconstruction | team science

Reconstruct was released more than twenty years ago as one of the first open-source image annotation applications that could be run on a personal computer (1–3). It offers a robust set of annotation features that are user-defined and field-agnostic. Since its release, additional annotation applications have followed, many written with connectomics-level analyses in mind (4–13). Modern applications have prioritized features that allow for rapid imaging and long-range automated segmentation of cell membranes to identify circuit connectivity (14–17). However, utilities needed for the detailed annotation and curation of synapses and subcellular features in the context of circuit-level analyses receive less attention.

Despite the many compelling features offered by the alternatives, Reconstruct continues to be used by a large and diverse group of researchers from a variety of fields. Reconstruct has been used to produce data in hundreds of publications ranging from neuroscience (18–24) to plant biology (25, 26), entomology (27–29), human anatomy (30), herpetology (31), and materials science (32), to name a few. We attribute its widespread use in part to Reconstruct's simple interface and flexible approach to annotation. Image stacks are imported into the application, and with little effort, researchers can quickly begin annotating serial sections, export data for analysis, and produce publication-quality 3D visualizations, all in a single intuitive application.

Despite significant advances in EM annotation tools, several fundamental challenges persist. Many require considerable programming expertise to access full annotation details and advanced features. This requirement limits accessibility to technical specialists rather than serving the broader research community. Most annotation tools lack robust, integrated systems for quality control and data curation. Many do not accommodate post hoc realignment of serial sections, making it difficult to correct alignment errors found during annotation or analysis. Finally, most tools separate metadata from image data, forcing researchers to maintain parallel data management systems and complicating long-term data preservation.

Significance

In neuroscience, the emerging field of connectomics has produced annotation tools for reconstruction that prioritize circuit connectivity across microns to centimeters and farther. Determining the strength of synapses forming the connections is crucial to understand function and requires quantification of their nanoscale dimensions and subcellular composition. PyReconstruct, successor to the early annotation tool Reconstruct, meets these requirements for synapses and other structures well beyond neuroscience. PyReconstruct lifts many restrictions of legacy Reconstruct and offers a user-friendly interface, integrated curation, dynamic alignment, nanoscale quantification, 3D visualization, and more. Extensive compatibility with third-party software provides access to the expanding tools from the connectomics and imaging communities.

Author contributions: M.A.C., J.N.F., and K.M.H. designed research; M.A.C., J.N.F., and K.M.H. performed research; M.A.C., J.N.F., M.D.M., and L.F.L. contributed new reagents/analytic tools; M.A.C. and J.N.F. analyzed data; and M.A.C., J.N.F., and K.M.H. wrote the paper.

Reviewers: H.B., Boston University; R.A.M., McGill; and P.K.R., Johns Hopkins Applied Physics Lab.

The authors declare no competing interest.

Copyright © 2025 the Author(s). Published by PNAS. This article is distributed under [Creative Commons Attribution-NonCommercial-NoDerivatives License 4.0 \(CC BY-NC-ND\)](#).

¹M.A.C. and J.N.F. contributed equally to this work.

²To whom correspondence may be addressed. Email: kharris@utexas.edu.

Published July 30, 2025.

*Some annotation tools do, however, include review modes, such as the review widget in CATMAID (4). This tool allows users to review skeletons and synapses in a systematic manner.

These limitations can significantly impede annotation workflows and compromise data integrity, particularly in large-scale projects.

Reconstruct has long been overdue for a major overhaul. It only ran natively on Windows machines, datasets were RAM-restricted in size, a complex system of transformations hampered new alignment strategies, and minimal interaction with outside tools restricted its expansion. Limitations like these required users to implement kludgy workarounds that complicated their workflows. Despite these limitations, Reconstruct continues to be used for its simplicity and efficiency.

With these limitations in mind, we have produced a generalizable and streamlined annotation tool in the spirit of Reconstruct that integrates readily into any serial imaging pipeline (Fig. 1). We have named this system PyReconstruct, a modern, user-friendly successor to what we now refer to as “legacy” Reconstruct. PyReconstruct was written in Python, retaining legacy Reconstruct’s intuitive interface and addressing the shortcomings necessary to transition from serial section to the volume electron microscopy needed for circuit analyses. It features an integrated curation system for maintaining data quality, flexible alignment capabilities, and unified data storage keeping meta-data and image data together. PyReconstruct runs on most operating systems, employs lightweight data structures, implements dynamic alignment, and provides multiresolution scaling. It lifts RAM restrictions allowing users to scale up to large volumes. PyReconstruct is also backward compatible with data annotated in legacy Reconstruct, giving legacy users the ability to port their data into the modern annotation environment. Importantly, PyReconstruct is fully open-source and users are at liberty to customize the source code to their own use cases.

User Experience

We designed the core functionalities and features of PyReconstruct to facilitate working with serial images in an unopinionated manner, to maintain data integrity, and to promote a collaborative workflow. In the sections below, we describe the annotation and manual segmentation interface, object organization capabilities, curation tools, alignment systems, and data visualization features.

Segmentation and Object Organization. PyReconstruct offers an uncomplicated graphical interface for registration, manual segmentation, and meshing of image data and allows for multiple points of entry and exit to and from third-party software (Fig. 2). By leveraging Python wrappers for openCV (4.8.1), stacks of serial 2D images can be loaded into PyReconstruct in multiple formats (.tiff, .jpeg, .png, etc.). Though PyReconstruct directly imports standard images without conversion, users can also benefit from its support of precomputed volume formats, the advantages of which are outlined below.

The user’s primary workspace contains a single image from the series (the “section”) displayed in the main window (Fig. 3A). The trace palette, tool bar, section navigator, and brightness/contrast sliders are superimposed over the image and are moveable around the field, such that the user can personalize their workspace as they annotate. Detachable windows display quantitative 2D (the trace list) and 3D annotation data (the object list) as it is being collected in the main window (Fig. 3B). Users are at liberty to choose trace name, color, tag, and appearance. The trace list allows users to view and edit traces on a section and see quantitative measurements, while the object list allows users to view and edit object data and see quantitative measurements in 3D based on the calibrated section thickness (1).

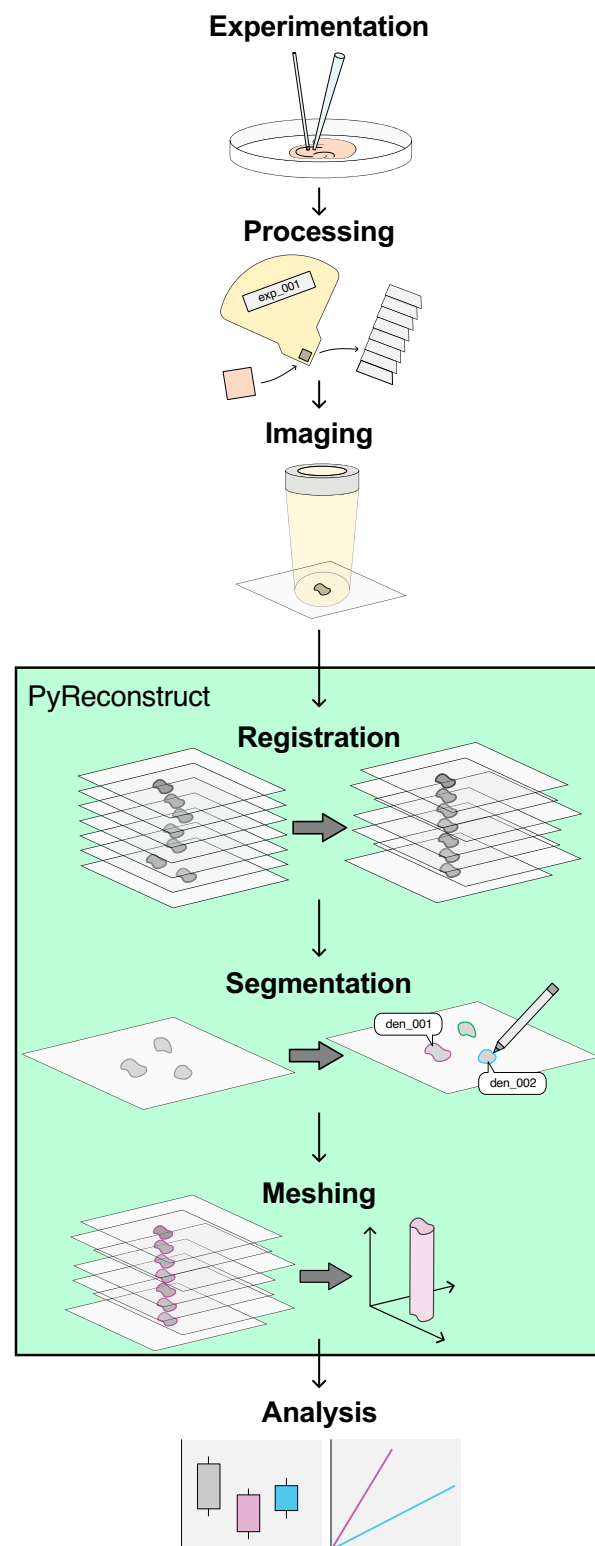


Fig. 1. Example serial imaging pipeline from experimentation through data analysis. PyReconstruct encompasses the most time-consuming steps (green box) in pipelines that rely on manual segmentation or proof reading of serial images to produce analyzable data. Here, a serial section EM pipeline is shown. Image registration, manual segmentation (generally referred to as “tracing” by laying down lines over membranes in EM images), and contour meshing can be performed in a single application. Images from any source can be used in this pipeline, including series or single sections.

In PyReconstruct, 3D “objects” represent collections of 2D “contours” over the image stack that belong to a single feature in the series. An object’s contour on a single section may consist of one or

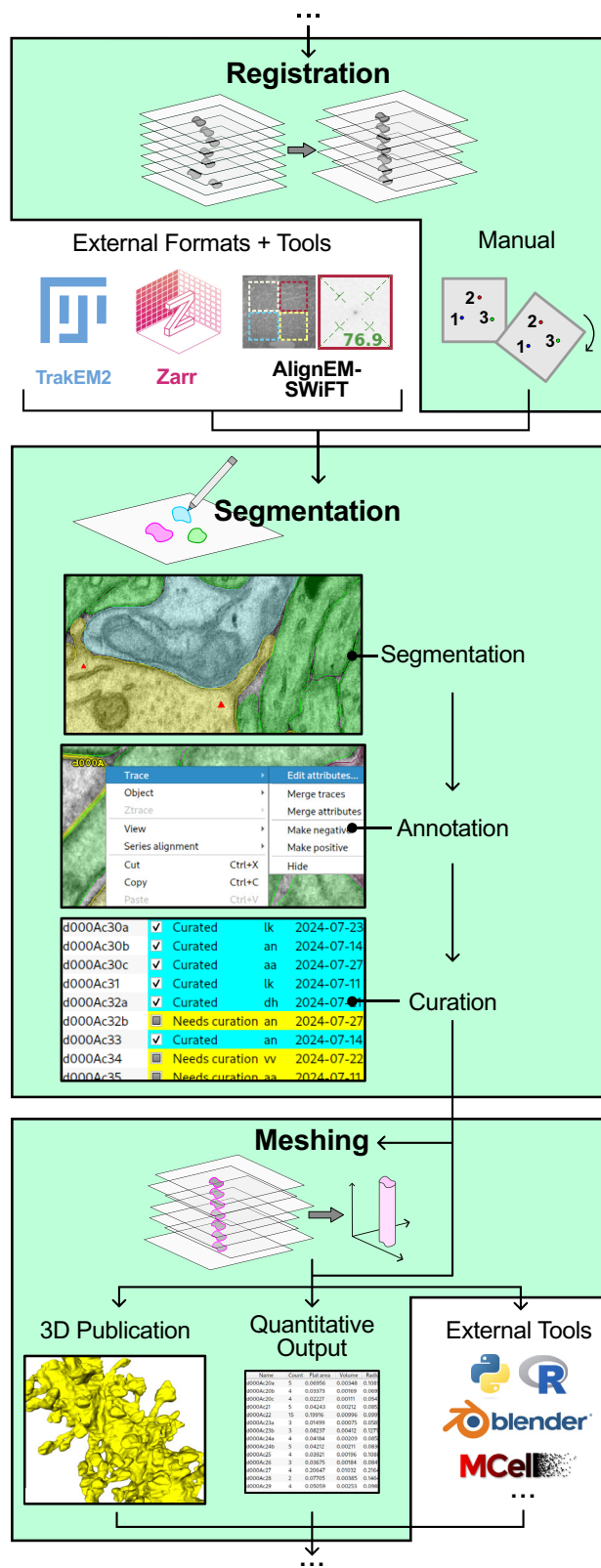


Fig. 2. PyReconstruct readily interacts with third-party software. Core PyReconstruct functions are highlighted in green and include native manual registration through the application interface, while also supporting importation of preregistered images and transformation matrices (6, 33, 34). PyReconstruct stores detailed segmentation data as 2D contours and features a checklist-based curation system for quality assurance. Users can generate, view, and export quantitative data and meshes directly in PyReconstruct to create publication-ready figures or for use externally in programming languages such as Python and R. Exported meshes can be further edited in advanced 3D platforms like Blender for biophysical modeling using programs like CellBlender and Mcell (35, 36).

several separate “traces” (Fig. 4A). Segmentation data in PyReconstruct are stored as lists of x and y positions that make up individual traces, and objects can be organized and classified in many ways. Hierarchical and nested objects groups can be created by assigning “hosts” that point to other objects. For example, “synapse” may point to “dendrite” and/or “axon”. Users can also create custom categories to assign objects qualitative measures. For example, “synapse” from the above example could also be categorized by “synapse type” as “excitatory” or “inhibitory”. For cases that fall outside host-inhabitant relationships and categorical variables, users can create simple, custom-named groups. Because these classification schemes are customizable, users can define semantically meaningful groups and relationships that are specific to their use-cases.

Rich, Free-Form Annotations and Event Tracking. PyReconstruct allows for rich annotations that might otherwise be stored externally and risk being separated from the original series. Annotations that provide metadata and context to series features can be applied to individual traces (tags), entire objects (groups and comments), and points of interest in the field (flags) (Fig. 4 B and C). For example, traces denoting object profiles distorted by image artifacts might be tagged to indicate that they have been interpolated (or inferred by the user) from traces on adjacent intact sections. Users may flag objects in a series that serve as probands or objects the annotator wishes to revisit later. Objects can be grouped to track their use in specific publications or projects, while comments provide additional explanatory notes. Free-form annotations like these enable users to create and customize their own annotation system based on project needs.

Experimentalists often revisit previously annotated series to test new hypotheses, and keeping track of the history of actions performed in a series may serve to guide subsequent annotation. In the past, this information was stored externally. PyReconstruct provides automation by logging all actions that add new or modify existing annotation data logged. Log entries contain brief descriptions of annotation events, including date, time, user, objects edited, and the section or sections on which the action was performed. Users can view and filter the full log to display entries relevant to one or more objects.

Collaborative Curation for Quality Control. Annotating large amounts of serial section data is generally performed among teams of annotators and PyReconstruct was developed with this approach in mind. Annotations performed by a team member are subsequently passed to a more expert annotator to be proofread and curated for quality assurance (Fig. 5). To this end, PyReconstruct includes a simple curation system, and users can be assigned curation tasks through the object list (Fig. 6A). Curation history (user, date assigned, completion status, etc.) is tracked with the series, so that project leads can verify whether annotation criteria is applied uniformly among team members and correct tracing errors. Curation data and history is readily available and displayed through the object list. Free-form annotations (Fig. 4 B and C) provide further context to aid collaboration among annotation teams. Field flags also include a running commentary that can be used to alert present and future annotators to information about locations in the series (Fig. 6B). Flag metadata including the creation time, username, and related notes are tracked and stored with series data. A conversation-style comment system allows users to maintain a running discussion for each flagged item. Tags applied to traces on a particular section can be accessed in a trace list (Fig. 6C), which when filtered and sorted, provides a rapid means to identify the status of a trace.

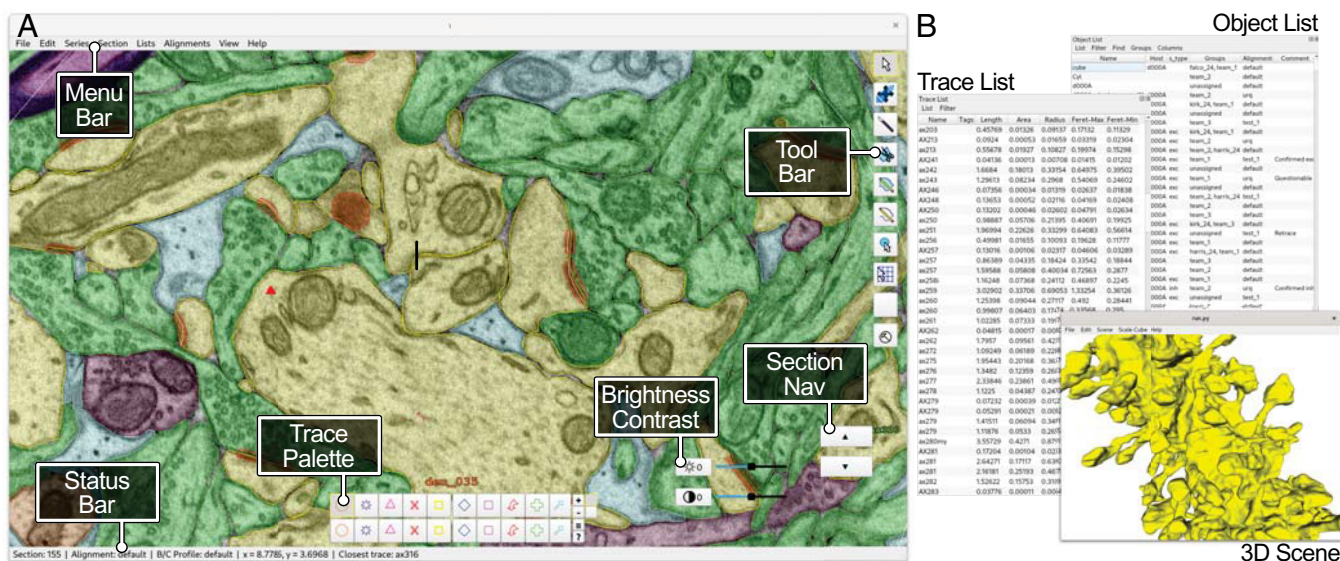


Fig. 3. Windowing schema in PyReconstruct. (A) The main window contains images and widgets (tools, trace palette, etc.) that can be moved around the frame and toggled on and off, allowing users to customize their primary workspace. (B) Users interact with 2D and 3D data as it is being collected through ancillary, detachable windows, such as the trace list, object list, and 3D scene.

PyReconstruct runs on a local machine and does not currently implement a client-server solution to allow multiple users to work simultaneously on a single series. Trace conflicts might therefore arise when series annotated simultaneously by different users are subsequently merged. For example, two annotators tracing the same object will lead to nonidentical, overlapping traces representing the same feature on a section. Merging large, heavily annotated series can result in many duplicate traces that pollute the workspace and lead to quantification errors.

To deal with this problem, a trace import system has been implemented in PyReconstruct that identifies and alerts users to merge conflicts that must be resolved. Conflicting traces are determined based on the Jaccard similarity coefficient, trace history, and annotator preference. Users can determine an overlap threshold above which traces are considered “identical enough”, which gives PyReconstruct leeway to discard all but one overlapping trace. This provides some automation to the tedious tasks of curating multiple traces for a single feature. Remaining conflicts are flagged for resolution, and users can walk through each conflict systematically.

Dynamic Alignments Applied on Demand. During processing, sectioning, and imaging, planar specimens are subjected to a variety of physical alterations (e.g., compression, shrinkage, heating) and technical complications (e.g., stage and specimen drift, nonuniform scan and lens characteristics) that introduce linear and nonlinear distortion into the final images (37–39). Image distortion can be mitigated through choice of processing protocol (40–43), imaging modality (44, 45), and post hoc computational processing, but in many cases must ultimately be corrected through image registration. Registration methods are rapidly improving (46–57), and choice in strategy depends on distortion type and personal preference. We therefore sought to implement a flexible and dynamic registration strategy to allow users 1) to import alignments generated externally, 2) to perform simple registration inside PyReconstruct, and 3) to store multiple alignments that can be applied to stacks of images on the fly (Fig. 7).

An “alignment” in PyReconstruct is represented by a list of affine transformations (Fig. 7A). Each section in the series is

associated with a single affine transformation, which is stored as a set of six numbers that correspond to the first two rows of the 2D transformation matrix. This single transformation is applied to both image pixels and contour data of a particular section, which are then displayed in the field when the section is called by the user. In this way, users whose images require affine transformations alone need not work with images whose alignments have been previously “baked in” (i.e., transformations applied directly to stored images).

This strategy offers several advantages. First, the only image data stored with a project are the unaligned images that were initially produced at the microscope and imported into PyReconstruct, dramatically reducing the size of a project. (Users can still of course use third-party software like Fiji, TrakEM2, and SWiFT-IR to import images with baked-in alignments and perform additional local alignments.) Second, stored contour points reflect the x and y positions of the points on the unaligned images (not the transformed images), making it possible for users to apply external transformations to those points when exporting contour data from PyReconstruct. Third, users can rapidly tweak a section’s alignment should they note alignment flaws while annotating, which is a common occurrence when working with serial images.

Finally, the simplicity of this strategy means users are at liberty to store multiple alignment profiles specific to an object, region of interest, or context, which can be applied to the series on demand (Fig. 7B). This is especially useful when annotating objects in areas of section deformation, for example, on either side of image artifacts (breaks, folds, tears, etc.), which are frequent in serial section EM. These artifacts would otherwise require users to use third-party image editing software to correct. Thus, a complete history of alignments for each series is stored. Objects in the series can be assigned to specific alignments, ensuring the object’s quantitative measurements and 3D reconstructions are accurate.

PyReconstruct supports simple manual alignment natively and users can interactively translate, rotate, scale, and shear images in the main window. Users can also directly edit a section’s affine transformation through the menu bar (Fig. 7C). Affine transformations can be estimated by identifying fiducial markers in the field, such as cell structures that span multiple sections. Transformations performed on single sections can be applied

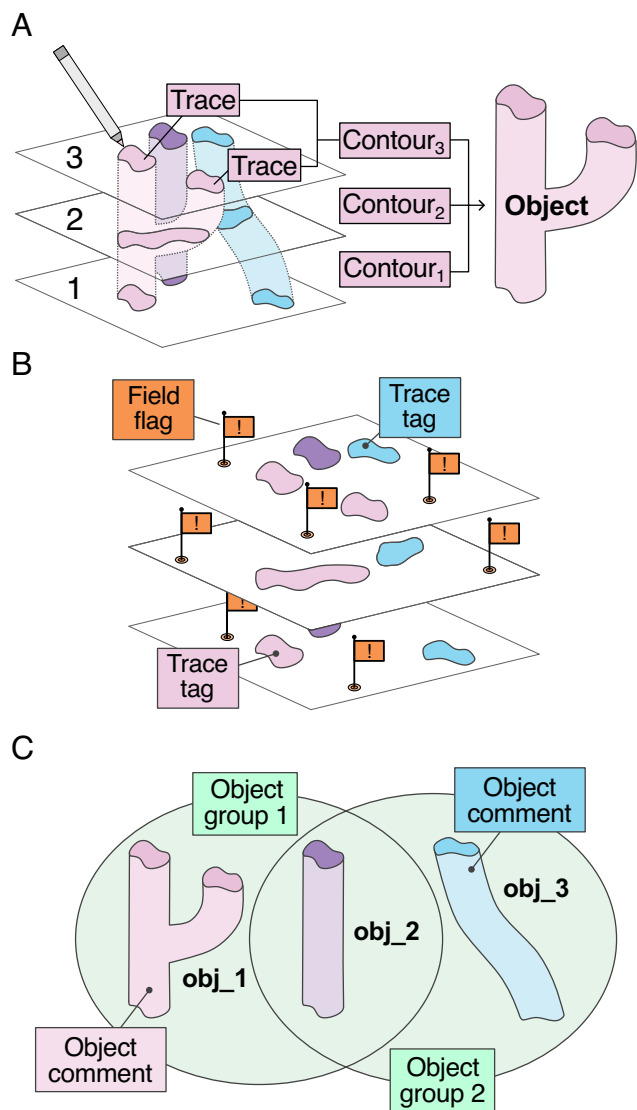


Fig. 4. PyReconstruct stores both free-form and hierarchically organized annotation data. (A) Object profiles on individual sections are identified and their outlines traced by annotators. An object's 2D contour consists of all traces on a section belonging to the object. 3D objects are constructed from multiple contours across serial images. (B) A trace tagging system allows users to ascribe additional information concerning 2D segmentations. (C) Annotations applied to objects include groups and comments, which can be accessed from the object list.

throughout the remaining sections, allowing for a correction in alignment to be propagated throughout the series. PyReconstruct supports importing alignments from other PyReconstruct projects as well as from external applications, for example, directly from SWiFT-IR project files (33, 56) or in the form of simple text files (.txt), each line representing an affine transformation.

Data Visualization and Analysis. PyReconstruct's object list represents a serialized view of objects, their measurements, and metadata and allows users to export data for analysis and render objects in 3D (Fig. 8). 2D contours are voxelized and represented as NumPy arrays, which are translated through a matrix-to-marching-cubes algorithm provided by the trimesh library (58) to generate watertight triangle meshes for visualization and quantification (Fig. 9A). The trimesh library provides several in-place smoothing filters (59, 60) that can be applied to meshes in PyReconstruct. 3D meshes are visualized in a customized 3D scene

built on top of the Python scientific visualization library vedo (61). The meshing strategies employed natively in PyReconstruct are modularized, such that users proficient in Python can implement more complex meshing algorithms accessible from the user interface should they choose to do so. 3D meshes can be exported from the object list in several formats (obj, ply, stl, etc.), which can be imported into external 3D modeling software, such as Blender, for further editing.

Segmentation issues are often not apparent when viewing objects as 2D profiles. Misalignments, poor manual segmentation, and misplaced traces become more evident when objects are rendered in 3D, and annotation quality is improved when users switch between 2D and 3D views while working. PyReconstruct's 3D scene includes several features to facilitate these actions. Double-clicking on a point in the 3D scene focuses on that point in the main window, providing a rapid way to identify 2D locations from the 3D space (Fig. 9B). Objects rendered in the 3D scene can be translated and rotated, allowing the user to customize the 3D view, for example, to visualize all objects of interest in a single glance (Fig. 9C). Objects from other series can also be imported into the current 3D scene. Customized 3D views can be saved as "scenes" that store object attribute and location information, which can be opened across annotation sessions. Scenes, in addition to aiding users in annotation, mitigate the need to export meshes to external 3D modeling software when making simple figures for publications.

Under the Hood

Interface Framework, Data Structures, and Legacy Compatibility.

PyReconstruct's user interface is powered by Python bindings for Qt6, an open-source and platform-independent framework for developing graphical user interfaces (62). Users can therefore run PyReconstruct on most major modern operating systems (Windows, macOS, and many Linux distros) right out of the box.

Annotation data in legacy Reconstruct were stored over multiple "trace files", one for each section, making moving series data between computers and users cumbersome and prone to data loss. Storing annotation data in a single, locally stored file facilitates data sharing among users. Annotation data in PyReconstruct are collected and stored in a single JSON-structured file with the extension .jsr (portmanteau of "JSON" and "series", pronounced "jay-sir", Fig. 10). Image data are stored separately in a format and location defined by the user.

The jsr file is divided into data pertaining to individual sections (section-specific data) and data pertaining to the entire series (series-specific data). Section-specific data contain contour information and annotations, transformations, and the section's image attributes (magnification, brightness, contrast, and image file pointer). Series-specific data store information that spans multiple sections, including, for example, series metadata, object attributes, current alignment, user information, and user preferences. All annotation data are accessible graphically through the application and through PyReconstruct's Python API.

PyReconstruct implements a composite file pattern approach when loading and saving data: Data stored in the single jsr file is decomposed at startup into discrete temporary hidden files that hold information pertaining to individual sections and the series. This approach optimizes RAM utilization while processing contour data and provides fault tolerance should the program unexpectedly close or the user's system fails.

Labs from a variety of fields continue to employ legacy Reconstruct as the primary tool used to annotate serial section

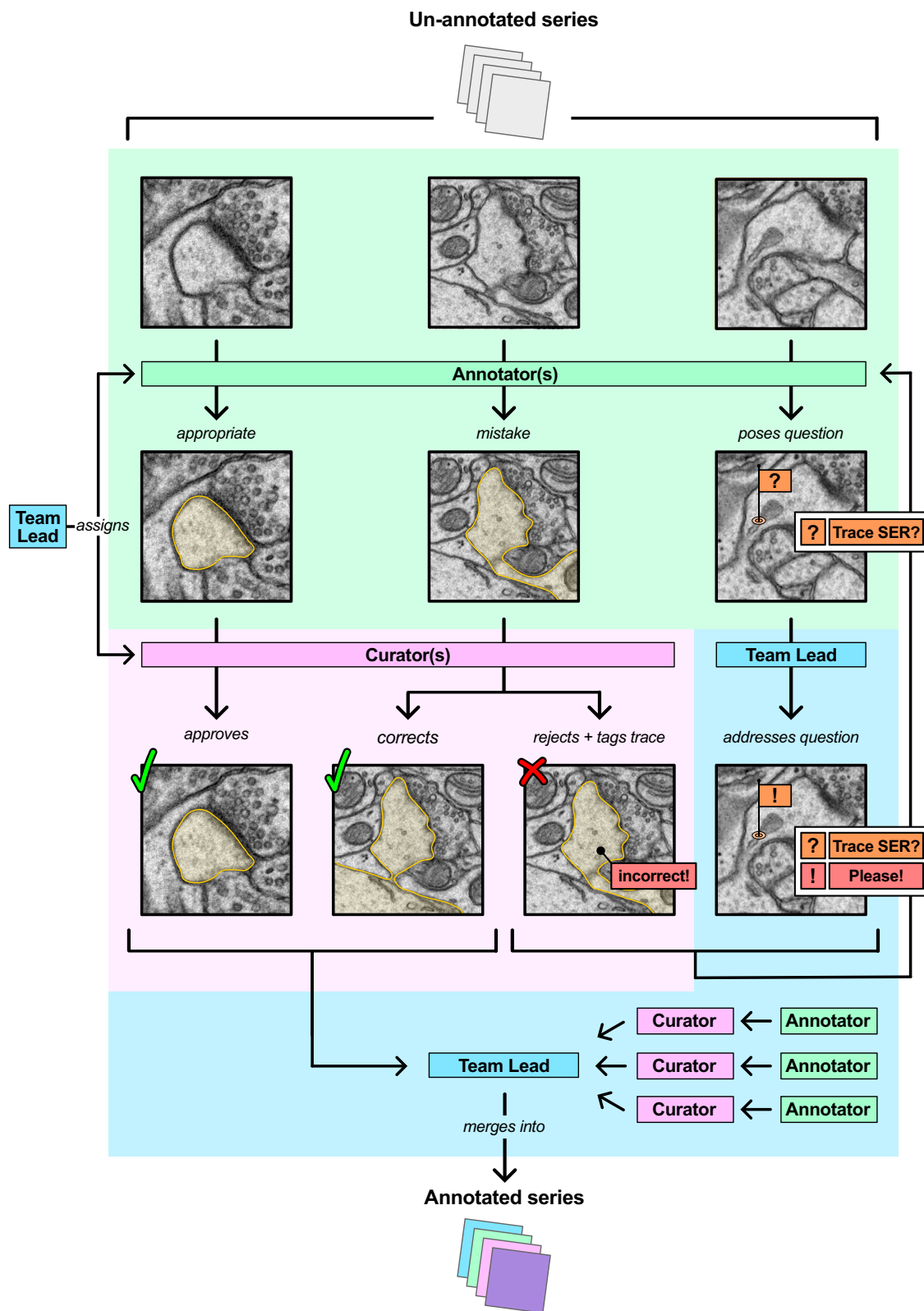


Fig. 5. Implementation of a team-based annotation and curation scheme to ensure quality control. A team lead (blue) assigns annotation (green) and curation tasks (pink) to team members working simultaneously on copies of a single series. Curators approve, correct, or reject traces, which can be tagged for review. Annotators can pose questions to team leaders through a system of flags with commentary that can be answered and returned. As annotations are curated, the partially annotated series can be passed back to the team lead. Curated series are merged into a single annotated dataset for analysis. PyReconstruct provides features at multiple steps in this pathway to facilitate curation and quality control.

EM data manually due in part to its ease of use. We therefore sought to make porting data from legacy Reconstruct into PyReconstruct simple. PyReconstruct is backward compatible with legacy structures: Series that were previously annotated in

Reconstruct and saved as XML can be loaded into PyReconstruct by simply pointing to the legacy structures. No external conversion is necessary. Importantly, this process is bidirectional: Annotation data collected in PyReconstruct can also be exported as legacy

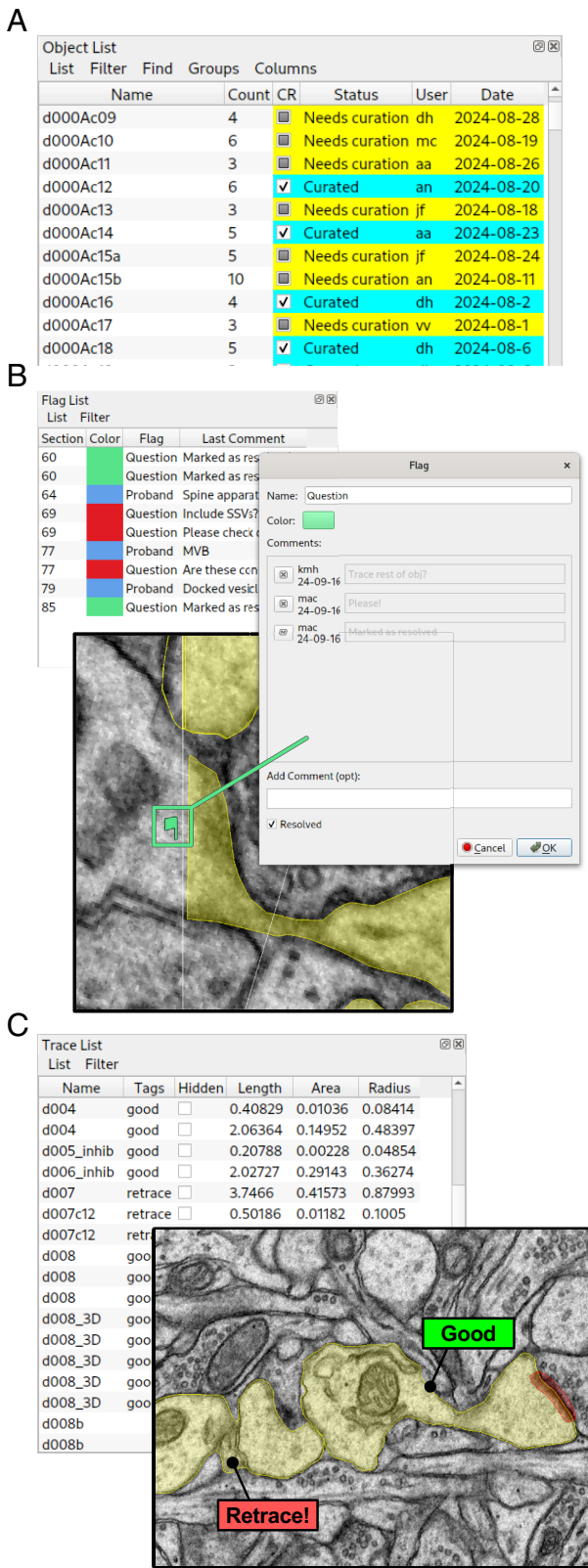


Fig. 6. PyReconstruct provides automation for curating segmentation data. (A) Tracking of curation tasks is stored with series data in PyReconstruct. Curation tasks and status can be assigned interactively to objects from the object list. Multiple filtering options allow users to view pending and completed curation tasks assigned to them and to others. Here, users were randomized to curation tasks through PyReconstruct's Python API. (B) Flags placed in the field are shown in a flag list, which can be sorted in various ways. Running commentary allows team members to pose questions and discuss issues that arise during annotation. (C) Traces can be tagged with information that is accessed from a sortable trace list. Here, an example trace incorrectly combines multiple adjacent structures and is tagged to alert users that the structures need to be retraced.

XML structures in case users have established workflows that rely on legacy structures remaining intact, for example, with neuropil tools (63). Features only compatible with PyReconstruct are saved in the jsr file. Users therefore retain full access to the legacy application should they choose to do so and can still benefit from PyReconstruct's modern annotation features.

Lifting RAM Restrictions through Multiresolution Scaling. In the past, we typically analyzed series of 200 to 250 TEM images ($4,000 \times 4,000$ px each), capturing high-resolution volumes measuring $\sim 10 \times 10 \times 12 \mu\text{m}$. Each 8-bit image (~ 16 MB) resulted in a full series of 3–4 gigabytes that could be annotated with ease in legacy Reconstruct. Over the past decade, however, we have adopted larger field imaging techniques (44, 45) and now routinely work with field sizes of $50 \times 50 \mu\text{m}$ (each image now ~ 600 MB). These datasets, reaching hundreds of gigabytes, exceed legacy Reconstruct's capacity and necessitated numerous workarounds that slowed the production of analyzable data. We therefore sought to overcome this limitation by implementing alternative data storage formats in PyReconstruct.

Datasets loaded in legacy Reconstruct could exceed RAM; however, two sections were loaded into memory simultaneously. This meant large images needed to be cropped to a size compatible with the user's RAM specs. Modern, ultra-large data viewers typically solve this issue by employing data structures that store chunked, compressed N-dimensional arrays at multiple resolutions (or "scales"), such as with HDF5 or Zarr. Precomputed image datasets can be manipulated through a variety of wrappers, such as h5py (64), PyTables (65), Z5 (66), and zarr-python (67). Instead of mapping entire images from disk into RAM, moving compressed chunks of data dramatically reduces loading times and makes navigating serial sections a much quicker and more pleasant experience. Saving the image data at multiple resolutions further reduces the amount of data loaded when users view low-magnification views of a section.

To lift legacy Reconstruct's RAM restrictions, we have implemented a multiresolution Zarr approach to loading and viewing image data in PyReconstruct. Zarr was chosen as it was designed specifically for Python, supports robust multithreading, provides access to customizable compressor and filter classes, and is used extensively in machine-assisted segmentation. Unlike applications that consolidate serial sections into a volumetric 3D Zarr, PyReconstruct implements a 2D layer approach: each section being stored as a separate annotated group, which allows users to switch between the original images and Zarr at will.

Storing and retrieving image data in a chunk-wise manner means PyReconstruct users are in practice no longer RAM-limited when annotating series. Users are now virtually unbounded by series size, restricted only by the disk space available on their local machines, which can be augmented with external and remote storage. This strategy permits near-instantaneous loading of images in the field, as only chunks at the lowest possible resolution based on zoom are loaded during viewing. PyReconstruct maintains its flexible alignment strategy by applying affine transformations nondestructively, only after image data are loaded. A multiresolution Zarr approach does increase the overall size of data stored per project, but PyReconstruct's scaling strategy means Zarr datasets are never heavier than 1.33 times the size of the original image stack.

As proof of principle, we montaged 20 tSEM images (each $\sim 50 \times 50 \mu\text{m}$ at a resolution of 2.5 nm/pixel) in a 2×10 pattern to create composite images $\sim 12 \text{ GB}$ measuring $100 \times 500 \mu\text{m}$. These images encompass areas exceeding the full dendritic arbor of a hippocampal CA1 pyramidal cell (stratum oriens to lacunosum

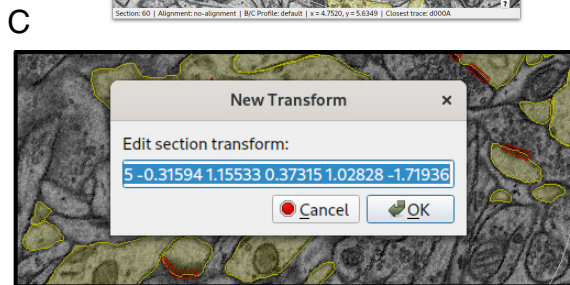
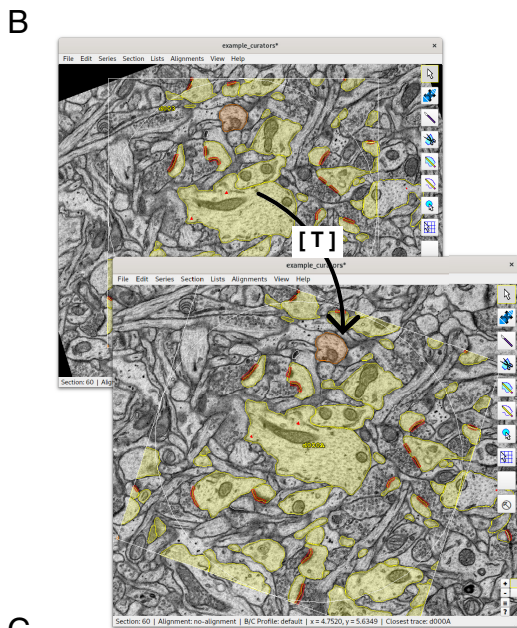
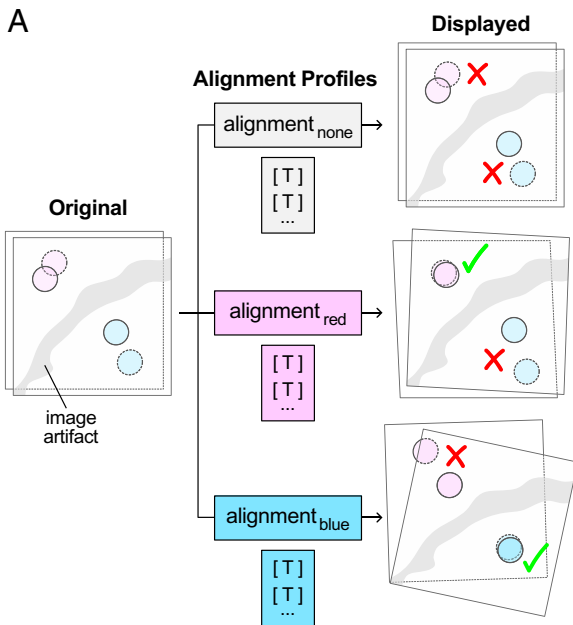


Fig. 7. Multiple alignment profiles applied to serial sections on demand. (A) PyReconstruct stores image and contour data in their untransformed state. Alignments are represented as lists of affine transformations ([T]), one for each section. Multiple alignments are stored as profiles that can be applied independently on demand. Image artifacts (resulting from tears, folds, etc. in serial sections) often warp serial sections and produce local misalignments. The ability to tweak, create, and store multiple alignments facilitates annotation. (B) Alignment profiles can be accessed and modified through the user interface. The current alignment is displayed by name in the main window's status bar (bottom of main window, see Fig. 3A). (C) New alignments can be created in PyReconstruct and imported from external applications or section transformations can be edited directly in the interface, allowing users fine control over series alignments.

molecular) and substantially surpass the size of standard 10×10 μm TEM images that we have used in the past. After converting to multiresolution Zarr format and loading into PyReconstruct, users could annotate neuropil structures with the same efficiency as when working with small-field images. This example provides a powerful demonstration of how Zarr implementation in PyReconstruct enables significant volume scaling without sacrificing performance on local machines.

Interacting with External Large-Image Applications and Datasets. Volumetric datasets are much larger than they used to be, even recently (68–73). This is due in part to the transition from volumes constructed from small-field TEM images to those from high-throughput methods such as focused ion beam SEM (74, 75), serial block face SEM (76, 77), and tape and array methods (78–81). Relying on manual segmentation alone is therefore increasingly unfeasible. However, many labs (including our own) continue to employ manual segmentation as a primary technique. We therefore sought to provide a simple platform that annotators can use to begin to interact with the many automated segmentation tools being developed by the connectomics community.

Neuroglancer is a WebGL-based application for viewing, annotating, and querying large, multiresolution volumetric data (82) and is the application of choice in several connectomics projects. Porting data to and from Neuroglancer offers one path through which automated segmentation efforts can be tapped into. PyReconstruct provides a graphical interface where users can export image data and contours as labeled Zarrs compatible with Neuroglancer. Data annotated in Neuroglancer can also be imported and converted to contour data for use in PyReconstruct.

Discussion

PyReconstruct provides solutions that enhance manual segmentation of serial images in a user-friendly and familiar interface and offers several advantages over legacy Reconstruct. The target audience includes researchers from a variety of largely unrelated fields, who rely on manual annotating serial sections and volume EM data. Thus, PyReconstruct is a nonspecialized tool offering platform-independence, simplified data structures, unique alignment strategies, and integration with external tools—now validated in recent studies (83, 84).

Integrated data quality control is often overlooked in annotation software, requiring users to develop their own external tracking systems. PyReconstruct has a robust and built-in curation system that addresses this critical gap. By embedding curation data directly within project files, PyReconstruct provides a streamed approach to team coordination and data integrity. PyReconstruct is fully open-source under a GNU General Public License v3 and users are encouraged to scrutinize and improve its source code, which is publicly available at GitHub (<https://github.com/synapseweb/pyreconstruct>). A user guide that includes step-by-step instructions on installing and launching PyReconstruct, starting a new series, and accessing a development version of the application is available at our lab's wiki site (<https://wikis.utexas.edu/display/khlab/PyReconstruct+user+guide>). This living document evolves with new tools and user strategies and is accessible via GitHub or directly within PyReconstruct through the “Online resources” section of the help menu.

Open-source tools like PyReconstruct empower users to create custom solutions that can be integrated into the main product to benefit the broader scientific community. Our team has already implemented several user-requested customizations: section randomization (and derandomization after tracing), the exportation

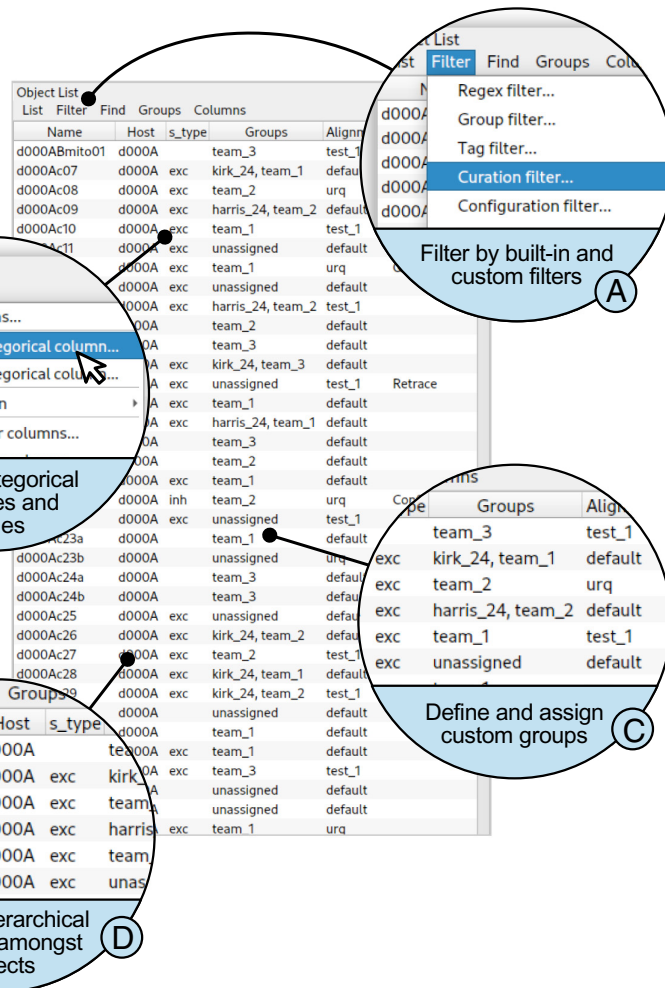


Fig. 8. Three-dimensional data are stored in the object list. Data concerning 3D objects constructed from 2D contours is displayed in the object list. Users can sort by built-in and custom filters (A), define categorical variables, and assign values (B), define and assign custom groups (C), and define hierarchical schema among objects by assigning objects as hosts (D).

of masks derived from traced objects for external automated classification schemes, and modifications to the interface that make tracing easier for left-handed users. These concrete examples showcase how the application’s open architecture facilitates adaptation to specific research needs. This open environment also makes it possible to develop data conversion strategies that allow PyReconstruct to accept annotations and segmentations from other systems.

As our understanding of alignment evolves, image registration strategies are advancing (46–57). The ability to realign a series means users can adapt and refine their work at all stages, rather than being constrained to a single baked-in alignment. Image flaws resulting in alignment errors are often not noticed until the annotation stage, when users are viewing sections at higher magnifications. The ability to tweak existing alignments rapidly and create new alignments when required therefore facilitates annotation and improves the quality of the 3D outcomes. In PyReconstruct, users are at liberty to align the series, import alignments from external software, and store multiple alignments that can be switched to and from on demand. Importantly, this strategy enables users to employ simple, nonelastic alignments in series that suffer from image artifacts that warp portions of a section (Fig. 7). Multiple alignment stacks for a single series and the ability to realign on demand also provide ground truth for developing more sophisticated automatic alignment methods.

Simplicity and generalizability come with tradeoffs. Fully segmenting, annotating, and curating EM volumes is time-consuming. For example, the complete manual annotation of a single, roughly $180\text{ }\mu\text{m}^3$ volume of hippocampal tissue—an exceedingly small volume by today’s connectomics standards—took a team of expert annotators more than a year to complete and curate using legacy Reconstruct (85). The process of scaling up is therefore impractical (if not impossible) when annotators rely on manual segmentation alone. The push by many teams to produce semi- and fully automated segmentation pipelines has led to the segmentation of breathtakingly large datasets (68–70, 72). Nevertheless, these pipelines remain largely relegated to specialist communities. Therefore, a need remains to adopt automated segmentation approaches in simple user interfaces for nonspecialist users.

One key challenge in adopting automated segmentation routines lies in balancing technical sophistication with accessibility. Modern automated segmentation tools require computational infrastructure and expertise in programming. The benefits of expanding access to these tools are immense. Moving forward, the developers of PyReconstruct are evolving its API and plugin framework to support the embedding of customized automated segmentation features into the software. This modular approach will enable researchers to leverage cutting-edge routines without the need for deep technical expertise, bridging the gap between specialist and nonspecialist communities.

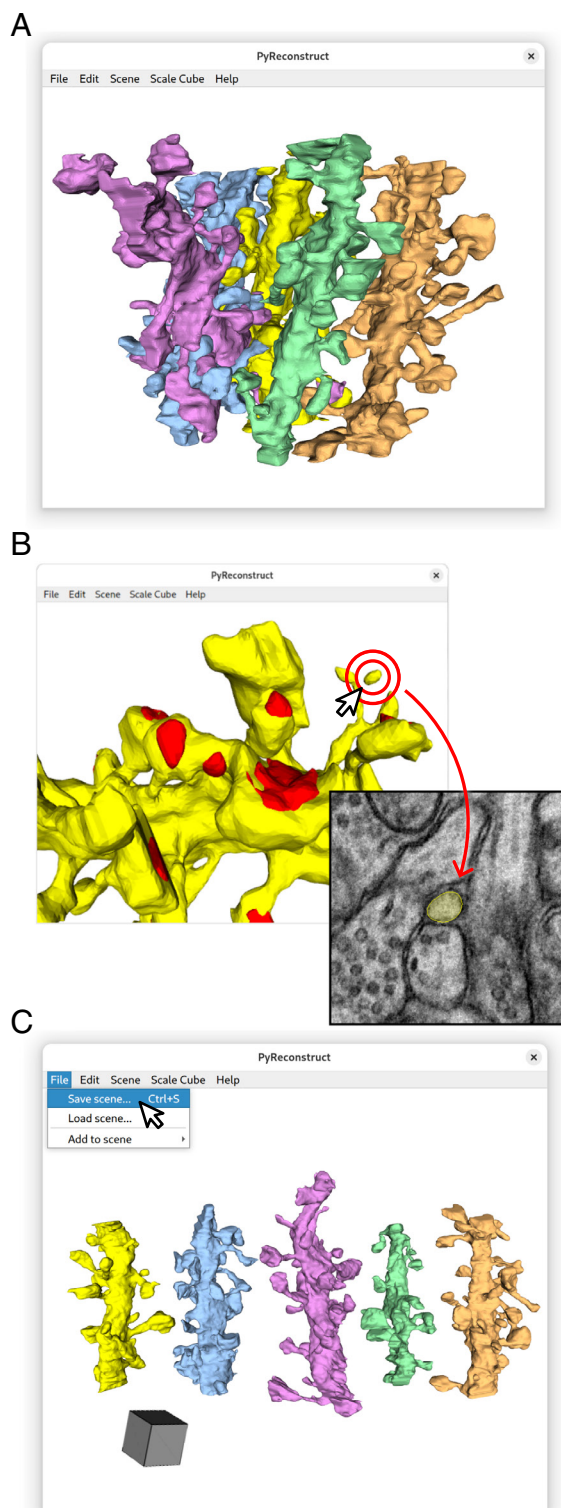


Fig. 9. An enhanced 3D scene facilitates detailed curation and stores publication-ready visualizations. (A) 3D renderings of objects can be generated from the object list and are displayed in a featureful 3D scene. (B) Double-clicking in the 3D scene focuses on the corresponding 2D location in the main window, allowing users to navigate to sections for curation. Here, a disconnected part of an object identified in the 3D scene is rapidly uncovered on the 2D section, allowing users to curate more finely the object's segmentations. (C) The updated 3D scene offers users features that organize objects in an automated fashion. Here, all objects in the 3D scene have been organized along a single axis, providing a visual overview of all meshes. Objects can be moved and rotated interactively and their attributes (color, opacity, etc.) can be altered. Scenes can be exported, saved, and reloaded at a later time, allowing users to produce publication-ready figures and store scenes with series data.

The evolution of imaging modalities over the past several decades has led to microscopy datasets that are larger than they have ever been (68–73, 86). These massive datasets have predominantly required server-based storage. Annotation tools that have grown up around these projects have therefore prioritized this approach (4, 9, 11). At present, PyReconstruct is a fully standalone application without server–client dependencies. Its users are not dependent on an internet connection, server maintenance, or remote data stores. While this approach offers simplicity and autonomy, users may need to generate manageable subvolumes from their data, especially when working with extremely large datasets that exceed local storage.

Previously, researchers faced the onerous task of manually cropping individual serial images. Today, the widespread adoption of chunk-wise data storage formats and the increasing availability of standardized, open-source databases for large image data (10, 87–90) have significantly mitigated these limitations. Users can efficiently extract subvolumes from remotely stored datasets through

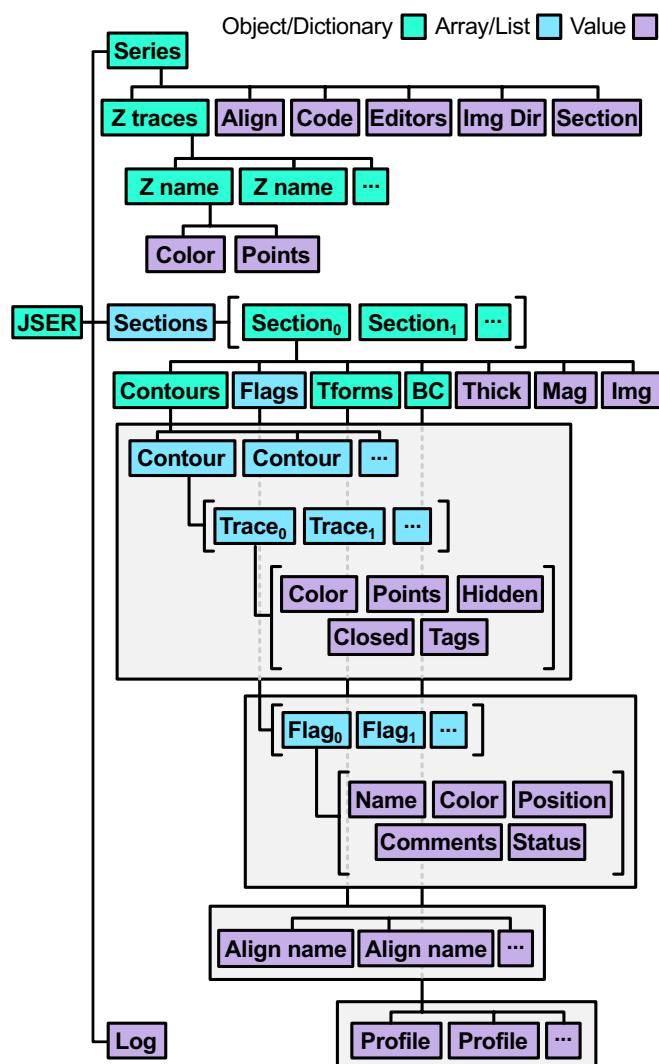


Fig. 10. Schematic of PyReconstruct annotation data. While legacy Reconstruct stored annotation data as multiple, noncanonical XML files, PyReconstruct stores annotation data locally as a single JSON-structured file (suffixed with .jsr) loaded as a Python dictionary and edited using built-in modules or through PyReconstruct's API. Series-wide data are held in a "Series" key, section data in a "Section" key, and series history in a "Log" key. The top-level key "Sections" maps to a list of section dictionaries with keys representing contour, flag, transformation data, etc. "Contours" is associated with a list of contours, which hold trace information. Traces are lists of trace attributes, such as trace color, points, visibility, etc. (Abbreviations: *Align* alignment, *Code* series code, *Img Dir* image directory, *Tforms* transforms, *BC* brightness/contrast profiles, *Thick* thickness, *Mag* pixel magnification, *Img* image file path.)

Python libraries like CloudVolume, which offer APIs to access pre-computed volumes (91). These tools can be readily integrated into a workflow to sample regions from larger volumes and use the suite of annotation, curation, quantification, and visualization features to produce high-quality data output from PyReconstruct.

Data, Materials, and Software Availability. All study data are included in the main text.

ACKNOWLEDGMENTS. We would like to thank Harris lab members, GitHub users, members of our regular PyReconstruct user meetings, and students in

NEU466G at the University of Texas at Austin for beta testing PyReconstruct and for their suggestions. Their input was vital in shaping the interface. We also would like to thank James Carson at the Texas Advanced Computing Center (TACC) for his help in integrating PyReconstruct with TACC's online access points and Vijay Venu Thiyagarajan for his suggestions regarding data structures. Funding: This work was supported by NIH Grants 1R56MH139176-01 and NSF Grants 1707356, 2014862, and 2219894 to K.M.H.

Author affiliations: ^aDepartment of Neuroscience, Center for Learning and Memory, The University of Texas at Austin, Austin, TX 78712

- J. C. Fiala, K. M. Harris, Extending unbiased stereology of brain ultrastructure to three-dimensional volumes. *J. Am. Med. Inform. Assoc.* **8**, 1–16 (2001).
- J. C. Fiala, Reconstruct: A free editor for serial section microscopy. *J. Microsc.* **218**, 52–61 (2005).
- Harris Lab SynapseWeb, (2025). <https://synapseweb.clm.utexas.edu> [Accessed 13 May 2025].
- S. Saalfeld, A. Cardona, V. Hartenstein, P. Tomancak, CATMAID: Collaborative annotation toolkit for massive amounts of image data. *Bioinformatics* **25**, 1984–1986 (2009).
- C. Sommer, C. Straehle, U. Köthe, F. A. Hamprecht, "Ilastik: Interactive learning and segmentation toolkit" in *2011 IEEE International Symposium on Biomedical Imaging: From Nano to Macro*, (IEEE, 2011), pp. 230–233.
- A. Cardona *et al.*, Trakem2 software for neural circuit reconstruction. *PLoS ONE* **7**, e38011 (2012).
- C. M. Schneider-Mizell *et al.*, Quantitative neuroanatomy for connectomics in *Drosophila*. *eLife* **5**, e12059 (2016).
- P. A. Yushkevich, Y. Gao, G. Gerig, ITK-SNAP: an interactive tool for semi-automatic segmentation of multi-modality biomedical images. *Conf. Proc. IEEE Eng. Med. Biol. Soc.* **2016**, 3342–3345 (2016).
- K. M. Boergens *et al.*, WebKnossos: Efficient online 3D data annotation for connectomics. *Nat. Methods* **14**, 691–694 (2017).
- T. Zhao, D. J. Olbris, Y. Yu, S. M. Plaza, NeuTu: Software for collaborative, large-scale. Segmentation-based connectome reconstruction. *Front. Neural Circuits* **12**, 101 (2018).
- D. R. Berger, H. S. Seung, J. W. Lichtman, VAST (Volume annotation and segmentation tool): Efficient manual and semi-automatic labeling of large 3D image stacks. *Front. Neural Circuits* **12**, 88 (2018).
- P. Hanslovsky *et al.*, Painter. Zenodo. (2024). 10.5281/zenodo.14454929. Deposited December.
- N. Sofroniew *et al.*, napari: a multi-dimensional image viewer for Python Zenodo. (2025). 10.5281/zenodo.14719463. Deposited 22 January.
- K. L. Briggman, D. D. Bock, Volume electron microscopy for neuronal circuit reconstruction. *Curr. Opin. Neurobiol.* **22**, 154–161 (2012).
- J. Kornfeld, W. Denk, Progress and remaining challenges in high-throughput volume electron microscopy. *Curr. Opin. Neurobiol.* **50**, 261–267 (2018).
- C. S. Xu, S. Pang, K. J. Hayworth, H. F. Hess, "Transforming FIB-SEM Systems for Large-Volume Connectomics and Cell Biology" in *Volume Microscopy* (Humana, New York, NY, 2020) pp. 221–243.
- C. J. Peddie *et al.*, Volume electron microscopy. *Nat. Rev. Methods Primers* **2**, 1–23 (2022).
- R. W. Castro, M. C. Lopes, L. M. De Biase, G. Valdez, Aging spinal cord microglia become phenotypically heterogeneous and preferentially target motor neurons and their synapses. *Glia* **72**, 206–221 (2024).
- D. Djama *et al.*, The type of inhibition provided by thalamic interneurons alters the input selectivity of thalamocortical neurons. *Curr. Res. Neurobiol.* **6**, 100130 (2024).
- K. Haruwaka *et al.*, Microglia enhance post-anesthesia neuronal activity by shielding inhibitory synapses. *Nat. Neurosci.* **27**, 449–461 (2024).
- D. Holl *et al.*, Distinct origin and region-dependent contribution of stromal fibroblasts to fibrosis following traumatic injury in mice. *Nat. Neurosci.* **27**, 1285–1298 (2024).
- M. K. P. Joyce, J. Wang, H. Barbas, Subgenual and hippocampal pathways in amygdala are set to balance affect and context processing. *J. Neurosci.* **43**, 3061–3080 (2023).
- Y. M. Morozov, P. Rakic, Disorder of golgi apparatus precedes anoxia-induced pathology of mitochondria. *Int. J. Mol. Sci.* **24**, 4432 (2023).
- M. Ziolkowska *et al.*, Phosphorylation of PSD-95 at serine 73 in dCA1 is required for extinction of contextual fear. *PLoS Biol.* **21**, e3002106 (2023).
- S. Amemiya *et al.*, Early stalked stages in ontogeny of the living isocrinid sea lily *Metacrinus rotundus*. *Acta Zool.* **97**, 102–116 (2016).
- J. L. Parke *et al.*, *Phytophthora ramorum* colonizes tanoak xylem and is associated with reduced stem water transport. *Phytopathology* **97**, 1558–1567 (2007).
- C. Groh, Z. Lu, I. A. Meinertzhagen, W. Rössler, Age-related plasticity in the synaptic ultrastructure of neurons in the mushroom body calyx of the adult honeybee *Apis mellifera*. *J. Comp. Neurol.* **520**, 3509–3527 (2012).
- M. A. Seid, E. Junge, Social isolation and brain development in the ant *Camponotus floridanus*. *Sci. Nat.* **103**, 1–6 (2016).
- J. Stöckl, G. Herzner, Morphology and ultrastructure of the allomone and sex-pheromone producing mandibular gland of the parasitoid wasp *Leptopilina heterotoma* (Hymenoptera: Figitidae). *Arthropod Struct. Dev.* **45**, 333–340 (2016).
- M. Baumgart *et al.*, Morphometric study of the two fused primary ossification centers of the clavicle in the human fetus. *Surg. Radiol. Anat.* **38**, 937–945 (2016).
- B. C. Moore, K. Mathavan, L. J. Guille, Morphology and histochemistry of juvenile male American alligator (*Alligator mississippiensis*) phallus. *Anat. Rec.* **295**, 328–337 (2012).
- C. M. Dinnis, A. K. Dahle, J. A. Taylor, Three-dimensional analysis of eutectic grains in hypoeutectic Al-Si alloys. *Mater. Sci. Eng. A, Struct. Mater. Prop. Microstruct. Process.* **392**, 440–448 (2005).
- SWIFT-IR. GitHub. (2023). Deposited 2023.
- J. Schindelin *et al.*, Fiji: An open-source platform for biological-image analysis. *Nat. Methods* **9**, 676–682 (2012).
- J. Stiles, T. Bartol, "Monte Carlo methods for simulating realistic synaptic microphysiology using MCell" in *Computational Neuroscience: Realistic Modeling for Experimentalists* (CRC Press, 2001), pp. 87–127.
- R. A. Kerr *et al.*, Fast monte carlo simulation methods for biological reaction-diffusion systems in solution and on surfaces. *SIAM J. Sci. Comput.* **30**, 24 (2008).
- T. Tasdizen *et al.*, Automatic mosaicking and volume assembly for high-throughput serial-section transmission electron microscopy. *J. Neurosci. Methods* **193**, 132–144 (2010).
- K. J. Hayworth *et al.*, Ultrastructurally smooth thick partitioning and volume stitching for large-scale connectomics. *Nat. Methods* **12**, 319–322 (2015).
- I. Lobato, T. Friedrich, S. Van Aert, Deep convolutional neural networks to restore single-shot electron microscopy images. *Npj Comput. Mater.* **10**, 1–19 (2024).
- H. Hillman, K. Deutsch, Area changes in slices of rat brain during preparation for histology or electron microscopy. *J. Microsc.* **114**, 77–84 (1978).
- B. Cragg, Preservation of extracellular space during fixation of the brain for electron microscopy. *Tissue Cell* **12**, 63–72 (1980).
- A. Schüz, G. Palm, Density of neurons and synapses in the cerebral cortex of the mouse. *J. Comp. Neurol.* **286**, 442–455 (1989).
- K. M. Harris *et al.*, Uniform serial sectioning for transmission electron microscopy. *J. Neurosci.* **26**, 12101–12103 (2006).
- M. Kuwajima, J. M. Mendenhall, L. F. Lindsey, K. M. Harris, Automated transmission-mode scanning electron microscopy (tSEM) for large volume analysis at nanoscale resolution. *PLoS ONE* **8**, e59573 (2013).
- M. Kuwajima, J. M. Mendenhall, K. M. Harris, Large-volume reconstruction of brain tissue from high-resolution serial section images acquired by sem-based scanning transmission electron microscopy. *Methods Mol. Biol.* **950**, 253–273 (2013).
- G. Balakrishnan, A. Zhao, M. R. Sabuncu, J. Guttag, A. V. Dalca, Voxelmorph: A learning framework for deformable medical image registration. *IEEE Trans. Med. Imaging* **38**, 1788–1800 (2019).
- S. Hamzehei *et al.*, 3D Biological/biomedical image registration with enhanced feature extraction and outlier detection. *ACM BCB* **2023**, 1 (2023).
- A. Hoopes, M. Hoffmann, B. Fischl, J. Guttag, A. V. Dalca, "HyperMorph: Amortized Hyperparameter Learning for Image Registration in Information Processing" in *Medical Imaging*, A. Fergan, S. Sommer, J. Schnabel, M. Nielsen, Eds. (Springer International Publishing, 2021), pp. 3–17.
- S. Klein, M. Staring, K. Murphy, M. A. Viergever, J. P. W. Pluijm, Elastix: A toolbox for intensity-based medical image registration. *IEEE Trans. Med. Imaging* **29**, 196–205 (2010).
- L. Liu *et al.*, "Learning by analogy: Reliable supervision from transformations for unsupervised optical flow estimation" in *2020 IEEE/CVF Conference on Computer Vision and Pattern Recognition (CVPR)*, (IEEE/CVF, 2020), pp. 6488–6497.
- E. Mitchell, S. Keselj, S. Popovych, D. Buniatyan, H. S. Seung, Siamese encoding and alignment by multiscale learning with self-supervision. *arXiv [Preprint]* (2019). <http://arxiv.org/abs/1904.02643> [Accessed 17 February 2025].
- S. Popovych *et al.*, Petascale pipeline for precise alignment of images from serial section electron microscopy. *Nat. Commun.* **15**, 289 (2024).
- S. Preibisch, S. Saalfeld, J. Schindelin, P. Tomancak, Software for bead-based registration of selective plane illumination microscopy data. *Nat. Methods* **7**, 418–419 (2010).
- S. Saalfeld, R. Fetter, A. Cardona, P. Tomancak, Elastic volume reconstruction from series of ultra-thin microscopy sections. *Nat. Methods* **9**, 717–720 (2012).
- J. Vargas, A.-L. Álvarez-Cabrera, R. Marabini, J. M. Carazo, C. O. S. Sorzano, Efficient initial volume determination from electron microscopy images of single particles. *Bioinformatics* **30**, 2891–2898 (2014).
- A. W. Wetzel *et al.*, "Registering large volume serial-section electron microscopy image sets for neural circuit reconstruction using FFT signal whitening" in *2016 IEEE Applied Imagery Pattern Recognition Workshop (AIPR)*, (IEEE, 2016), pp. 1–10.
- T. Xin *et al.*, A novel registration method for long-range serial section images of EM with a serial split technique based on unsupervised optical flow network. *Bioinformatics* **39**, btad436 (2023).
- Trimesh Dawson-Haggerty (2023). Deposited 2023.
- M. Desbrun, M. Meyer, P. Schröder, A. H. Barr, "Implicit fairing of irregular meshes using diffusion and curvature flow" in *Proceedings of the 26th Annual Conference on Computer Graphics and Interactive Techniques, SIGGRAPH '99*, (ACM Press/Addison-Wesley Publishing Co., 1999), pp. 317–324.
- J. Vollmer, R. Mend, H. Müller, Improved laplacian smoothing of noisy surface meshes. *Comput. Graph. Forum* **18**, 131–138 (1999).
- M. Musy *et al.*, <https://doi.org/10.5281/zenodo.8067437>. (2023) Deposited 21 June 2023.
- O Project, Qt6. (2025). Deposited 2025.
- Cell Blender, MCell Team GitHub. (2022). Deposited, 2022.
- A. Collette, *Python and HDF5* (Unlocking Scientific Data O'Reilly, 2013).
- PyTables Developers Team, PyTables: Hierarchical datasets in Python. (2025). Accessed 13 May 2025.
- C. Pape *et al.*, Z5. Zenodo. <https://doi.org/10.5281/zenodo.11671609>. Deposited 15 June 2024.
- A. Miles *et al.*, Zarr-Python. Zenodo. 10.5281/zenodo.14873428. Deposited 14 February 2025.
- A. Shapson-Coe *et al.*, A petavoxel fragment of human cerebral cortex reconstructed at nanoscale resolution. *Science* **384**, eadk4858 (2024).
- A. Azevedo *et al.*, Connectomic reconstruction of a female *Drosophila* ventral nerve cord. *Nature* **631**, 360–368 (2024). 10.1038/s41586-024-07389-x.
- S. Dorkenwald *et al.*, Neuronal wiring diagram of an adult brain. *Nature* **634**, 124–138 (2024).

71. J. A. Bae *et al.*, Functional connectomics spanning multiple areas of mouse visual cortex. *Nature* **640**, 435–447 (2025).
72. N. L. Turner *et al.*, Reconstruction of neocortex: Organelles, compartments, cells, circuits, and activity. *Cell* **185**, 1082–1100.e24 (2022).
73. L. K. Scheffer *et al.*, A connectome and analysis of the adult *Drosophila* central brain. *eLife* **9**, e57443 (2020).
74. J. A. W. Heymann *et al.*, Site-specific 3d imaging of cells and tissues with a dual beam microscope. *J. Struct. Biol.* **155**, 63–73 (2006).
75. G. Knott, H. Marchman, D. Wall, B. Lich, Serial section scanning electron microscopy of adult brain tissue using focused ion beam milling. *J. Neurosci.* **28**, 2959–2964 (2008).
76. S. B. Leighton, SEM images of block faces, cut by a miniature microtome within the SEM - A technical note. *Scan Electron Microsc.* 73–76 (1981).
77. W. Denk, H. Horstmann, Serial block-face scanning electron microscopy to reconstruct three-dimensional tissue nanostructure. *PLoS Biol.* **2**, e329 (2004).
78. K. D. Micheva, S. J. Smith, Array tomography: A new tool for imaging the molecular architecture and ultrastructure of neural circuits. *Neuron* **55**, 25–36 (2007).
79. R. Schalek *et al.*, Development of high-throughput, high-resolution 3D reconstruction of large-volume biological tissue using automated tape collection ultramicrotomy and scanning electron microscopy. *Microsc. Microanal.* **17**, 966–967 (2011).
80. H. Horstmann, C. Körber, K. Sätzler, D. Aydin, T. Kuner, Serial section scanning electron microscopy (S3EM) on silicon wafers for ultra-structural volume imaging of cells and tissues. *PLoS ONE* **7**, e35172 (2012).
81. K. J. Hayworth *et al.*, Imaging ATUM ultrathin section libraries with WaferMapper: A multi-scale approach to EM reconstruction of neural circuits. *Front. Neural Circuits* **8**, 68 (2014).
82. J. Maitin-Shepard *et al.*, Neuroglancer: Web-based volumetric data visualization Zenodo. (2021). 10.5281/zenodo.5573294. Deposited 16 October.
83. L. M. Kirk *et al.*, Presynaptic vesicles supply membrane for axonal bouton enlargement during LTP. *bioRxiv* [Preprint] (2025). <https://www.biorxiv.org/content/10.1101/2025.04.29.651313v2> [Accessed 13 May 2025].
84. G. C. García *et al.*, The presynaptic vesicle cluster transitions from a compact to loose organization during long-term potentiation. *bioRxiv* [Preprint] (2024). <https://www.biorxiv.org/content/10.1101/2024.11.01.621529v1> [Accessed 13 May 2025].
85. K. M. Harris *et al.*, A resource from 3D electron microscopy of hippocampal neuropil for user training and tool development. *Sci. Data* **2**, 150046 (2015).
86. N. Kasthuri *et al.*, Saturated reconstruction of a volume of neocortex. *Cell* **162**, 648–661 (2015).
87. J. T. Vogelstein *et al.*, A community-developed open-source computational ecosystem for big neuro data. *Nat. Methods* **15**, 846–847 (2018).
88. W. T. Katz, S. M. Plaza, DVID: Distributed versioned image-oriented dataservice. *Front. Neural Circuits* **13**, 5 (2019).
89. C. S. Xu *et al.*, An open-access volume electron microscopy atlas of whole cells and tissues. *Nature* **599**, 147–151 (2021).
90. R. J. Hider *et al.*, The brain observatory storage service and database (BossDB): A cloud-native approach for petascale neuroscience discovery. *Front. Neuroinform.* **16**, 828787 (2022).
91. W. Silversmith *et al.*, Igneous: Distributed dense 3D segmentation meshing, neuron skeletonization, and hierarchical downsampling. *Front. Neural Circuits* **16**, 977700 (2022).